INSTITUTE OF PLASMA PHYSICS

NAGOYA UNIVERSITY

IMPURITY ORIGIN DURING ICRF HEATING IN JIPP T-IIU TOKAMAK

N. Noda, T. Watari, K. Toi, E. Kako, K. Sato, K. Ohkubo,
K. Kawahata, I. Ogawa, T. Tetsuka, S. Tanahashi, S. Hirokura,
Y. Taniguchi, Y. Kawasumi, R. Ando, and J. Fujita

(Received – June 7, 1984)

IPPJ- 682 June 1984

RESEARCH REPORT

NAGOYA, JAPAN

IMPURITY ORIGIN DURING ICRF HEATING IN JIPP T-IIU TOKAMAK

N. Noda, T. Watari, K. Toi, E. Kako, K. Sato,
K. Ohkubo, K. Kawahata, I. Ogawa, T. Tetsuka,
S. Tanahashi, S. Hirokura, Y. Taniguchi,
Y. Kawasumi, R. Ando, and J. Fujita

(Received - June 7, 1984)

IPPJ- 682 June 1984

Revised manuscript of the paper 5 - 4 presented at the 6th International Conf. on Plasma Surface Interactions in Controlled Fusion Devices (Nagoya, Japan, May 14 - 18, 1984)
to be published in *J. Nuclear Materials, North-Holland Publishing Co. Amsterdam*

Further communication about this report is to be sent to the Research Information Center, Institute of Plasma Physics, Nagoya University, Nagoya 464, Japan.

ABSTRACT

Replacing stainless steel limiters by graphite limiters, we found that radiations from iron and titanium ions were significantly reduced. Total radiation and loop voltage also decreased. This indicates the limiters are the major impurity sources both in Ohmic and rf heating phases. Although titanium radiations increased with rf power injected by an antenna with titanium Faraday shield, the maximum intensity was much smaller than those in experiment where the titanium-flashed stainless steel limiters were used. Thus it has been found that Faraday shield is less important as an impurity source than limiters. Toroidal asymmetry observed for OII radiations suggests that the energetic charge-exchange neutrals play a role in releasing oxygen from the wall and that those energetic particles are relatively abundant in the toroidal sections near the antenna.

The radiation $H_\alpha + D_\alpha$ decreases during rf pulse around the limiter, which may be due to the change in hydrogen/deuterium recycling at the limiter. The reduction of $H_\alpha + D_\alpha$ is greater with graphite limiters than with stainless steel limiters. The relation between recycling and impurity release is briefly discussed.

1. INTRODUCTION

High frequency-wave heating is one of the promising techniques of further heating in future large tokamaks. Wave heating at ion-cyclotron range of frequencies (ICRF) is especially attractive because it shows a good efficiency for ion heating.[1-4] It has been reported, however, that rf heating causes relatively large amount of impurity contamination compared to other heating techniques.[5,6] The impurity contamination makes the plasma column unstable and the maximum input power is often limited by disruption due to peaking of the current distribution caused by radiation cooling in peripheral region. It has been also observed that the central electron temperature goes down during ICRF pulse.[1,4] Thus, for successful rf heating, it is important to understand the mechanism which dominates the impurity generation and to find a method to reduce the impurity contamination. As the first step of the impurity study, we have carried out a series of ICRF heating experiments with JIPP T-IIU tokamak, especially focusing our attention on identification of impurity origin.

2. EXPERIMENTAL SETUP

JIPP T-IIU is a tokamak device constructed by modifying the

JIPP T-II stellarator/tokamak. The major radius of the vacuum vessel is 93 cm and the minor radius is 32 cm. The plan view of JIPP T-IIU is shown in Fig.1. It has 20 toroidal coils and each toroidal section is numbered as P1, P2 ... P20 in the figure. Two sets of poloidal limiters are mounted at sections P7 and P17. Three antennas on high field side were used as ICRF launchers in this series of experiments. These antennas are located at P4, P14 and P15. The device has two bellows sections and, on each side of the bellows section, auxiliary limiters are set as a bellows guard. In Fig.2 is shown a sectional view of the vacuum vessel. Usually the center of plasma-current channel is feedback-controlled to locate at R = 91 cm. The minor radius of the plasma is limited to 22.5 cm by the inner limiters. The minor radius of the guard limiters, which are not shown in Fig.2, is 25 cm. The vacuum vessel, the main limiters and Faraday shields are made of stainless steel SUS 304. The guard limiters are made of molybdenum. During these experiments, both sets of the main limiters were replaced by graphite limiters of the same shape and size. The Faraday shield was also changed to a titanium one. Titanium gettering was applied in the course of the experiments with the stainless steel (SUS) limiter. The locations of Ti ball are also shown in Fig.1. Hydrogen and impurity radiations were measured and their variations were compared each other. Toroidal variation of $H_\alpha + D_\alpha$ line radiation and that of OII 4415 Å were studied by means of a

simple device consisting of an interference filter and a photodiode. The full width at the half maximum of the filters is 30 A , which is narrow enough to separate the H_α + D_α or OII lines from other radiations. A grazing incidence spectrometer was used at P6 for measurements of the radiation in vacuum ultraviolet region. Total radiation intensity was monitored with pyroelectric detectors and metallic bolometers. A set of two Langmuir probes are on the section P8 and the distances from the axis of the vacuum vessel are 27 and 28 cm.

3. RESULTS AND DISCUSSIONS

3.1 Parameters of Target Plasmas and ICRF Heatings

This series of experiments was concentrated on a hydrogen-minority heating with antennas on high field side and the toroidal field B_0 of 2.94 T (see Fig.2). A mixture of 10% H_2 and 90% D_2 is used. Typical plasma parameters are tabulated in Table 1. The loop voltage necessary for the same plasma current with the graphite limiters was a half of that with the SUS limiters. Thus, the plasma resistivity is significantly reduced by using the graphite limiters even in the Ohmic heating phase. The impurity radiations with the graphite limiters were compared to those with the SUS limiters under the conditions where the Ohmic input power of the target plasmas was almost equal. The

applied rf frequency is 38.5 MHz for P4 antenna and 40.0 MHz for P14 and P15 antennas. The maximum rf power absorbed by the plasma is 400 kW per each antenna. In an optimized case with the SUS limiters, rf power as large as 500 kW could be injected without causing any minor disruption. The ion temperature and the electron temperature rose up to 1.1 keV in this case. Electron-heating efficiency was greater with the graphite limiters than with the SUS limiters and the electron temperature went up to as high as 1.8 keV with 250 kW rf injection.

3.2 Effects of Limiter Materials

The impurity study has been carried out for rf power levels up to 300 kW. Figure 3 shows relative changes of impurity radiations as a function of rf power. The radiation intensities with the SUS limiters and with the graphite limiters are plotted. It is clearly seen that the radiations from iron and titanium ions are significantly reduced by using the graphite limiters. The titanium-gettering had been applied 3 months before the mesurements of the radiations in Fig.3. Both SUS limiters were covered with titanium on their electron sides (see the location of Ti balls in Fig.1). A significant decrease in Ti VIII indicates that most of titanium impurity was generated from the SUS limiters covered with titanium. The radiations from the impurities of limiter materials increased with rf power and did

not reach saturation within this power level.

The measurements with the graphite limiters were done using the P4 antenna with a Faraday shield made of titanium. Although the titanium radiation increases with rf heating by a factor of 5, the radiation intensity is still much smaller than that obtained with the titanium-flashed SUS limiters. As is shown in Fig.2, the front surface of the Faraday shield is 11 mm behind the front of the main limiter. The results shown in Fig.3 indicate that, under such conditions, impurity generation on the Faraday shield is less important than that on the limiter. This conclusion is similar to that obtained for H-minority heating in PLT.[7] On the other hand, this is different from the results obtained in TCA tokamak with the Alfven wave heating, where the main origin of impurities is concluded to be rf-antennas.[6] This difference is thought to be due to the fact that the heating mechanisms are quite different in ICRF heating and Alfven wave heating. The intensity of CIV increased by a factor of two with the graphite limiter, compared to that in the SUS limiter, both in Ohmic and ICRF heating phases. We think that the difference in the CIV intensities shown in Fig.3 is the net increase caused by introducing the graphite limiters. It should be noted, however, that the signal of CIV with SUS limiters is possibly blended with some impurity radiations other than carbon and then the net intensity of CIV is not clear in this case.

The total radiation measured with bolometers was 500 kW in

Ohmic phase with the SUS limiter and decreased to 260 kW when graphite was used. A considerable amount of molybdenum radiation was observed in discharges with the SUS limiter. Both the iron and the molybdenum radiations may be responsible for the total radiation in the discharges with the SUS limiter. The intensity of the molybdenum radiation decreased with the graphite limiters by a factor of 8, compared to that with the SUS limiters.

3.3 Effect of Titanium Gettering with SUS Limiters

Titanium gettering was once applied in the course of the experiments with the SUS limiters. In Fig.4 the radiations of OV and Ti VIII are compared for the discharges before and after the gettering. The gettering was applied for the first time between the discharges of shot Nos. 10726 and 10727. The Ti ball of P14 section was used and about 20 mg of Ti was flashed. Figure 4(a) shows that the increase in the oxygen radiation during rf heating was suppressed by this first trial of gettering. The gettering was applied in every interval of discharges after shot No.10735. After several tens of discharges, the oxygen radiation was significantly reduced. In the course of the repetitive gettering, titanium radiations gradually increased up to the levels shown in Fig.4(b).

It was found that the electron density n_{es} in the scrape-off layer also increased during rf heating. Before the

gettering, the density with the rf heating was 5 times larger than that in Ohmic phase. After the gettering, the density-increase rate was reduced to be 1.6, indicating that the density-increase in the scrape-off layer strongly correlated with the increase of the oxygen radiations. Considerable part of the increased electrons probably came from oxygen.

The iron impurity radiation was not much reduced and still determined the plasma properties. The plasma parameters such as loop voltage, n_e, T_e, T_i, *etc.* did not change by the gettering. The influence of the increased titanium on the plasma property is not clear.

3.4 Behavior of OII and H_α + D_α Radiations

The radiation OII 4415 A showed no significant toroidal asymmetry in Ohmic heating phase. This suggests that oxygen originates from a broad area of the first wall. With the SUS limiters, we found a clear toroidal asymmetry in OII intensity during rf heating. Typical results are shown in Fig.5. Figure 5(a) shows the behaviors of OII at P6, P8, P13 and P16 sections with rf power of 150 kW launched from the antenna at P4. The radiation increase is clearly seen only at P6 and P8, which are closer to the antenna than P13 and P16. On the other hand, Fig.5(b) shows that the increase in OII is largest at P13, which is just next to the antenna used. These results indicate that

the oxygen influx is relatively large in the region close to the antenna. This can be interpreted as follows: i) Oxygen is released from the first wall by charge exchange neutrals. ii) By ICRF heating, the energy and particle-flux intensity of the neutrals and ions are increased. iii) Absorption of rf power is toroidally localized in the vicinity of the antenna. iv) Ions are accelerated perpendicularly and a considerable part of accelerated ions is also localized as trapped ions, which results in relatively high density of energetic ions around the antenna region.

In case of using the graphite limiter, the limiter can be another important source of oxygen. Different from the case with the SUS limiter, the intensity of OII was not small at P16 even though the P4 antenna was used. In Fig.6, typical results obtained with the graphite limiters are shown. As for the OII radiation, the following points are remarkable: i) The increase in OII radiation is large at a toroidal location close to the limiter and far apart from the antenna. ii) The rise time of OII with the rf heating is longer than that in the case of using SUS limiters. iii) The intensity level is higher after the rf power is off than that before injection. These are not found with the SUS limiters and suggest some chemical processes which release oxygen from the graphite limiter.

In Fig.6, the behavior of H_α + D_α radiation are also shown. After initiation of the discharge, the radiation increases

significantly at P16 as the plasma column is shifted inward. As the detector at P16 looks directly at the inner limiter surface, this increase shows that strong hydrogen and deuterium recycling takes place there. It is clearly seen that the radiation decreases during the rf heating. The plasma position is feedback-controlled and does not shift outward. This decrease is presumed to be due to change of recycling. As is shown in section 3.5, the electron temperature in the scrape-off layer rises during the rf heating and this can be a main reason which reduces the recycling. This causes the increase of the surface density of H and D on the graphite limiter, which results in oxygen and carbon release through chemical processes.

It should be noted that the $H_\alpha + D_\alpha$ signal at P6 is small in the recycling phase in Fig.6. This is because the line of sight at P6 was not directly on the inner limiter at P7 but more than 10 cm away from the limiter. Here we can see that the $H_\alpha + D_\alpha$ radiation increases during the rf heating. It has been also observed that $H_\alpha + D_\alpha$ increases at P13 when the antenna at P14 is used as the rf launcher. During the rf heating the $H_\alpha + D_\alpha$ radiation usually increases at the location close to the antenna. Here is another mechanism of hydrogen/deuterium recycling different from that on the limiter, and it may have a relation to charge-exchange neutrals of high energy component generated by the rf heating.

3.5 Electron Density and Temperature in the Scrape-Off Layer

Plasma parameters in the scrape-off layer are important because they may have close relations to impurity behaviors. Electron density n_{es} and temperature T_{es} in the scrape-off layer were measured as a function of rf power. The results are shown in Fig.7. The probe was located at 27 cm from the axis of the vessel. The center of the plasma-current was at R = 91 cm and the minor radius of the plasma was 22.5 cm. Thus, the probe was located at r = 6.5 cm from the plasma edge.

In Table 2, typical values of n_{es} and T_{es} are shown. In Ohmic heating phase, n_{es} at r = 6.5 cm was 5.4×10^9 cm^{-3} for the plasma densities $\overline{n_e} = 2.5 \times 10^{13}$ cm^{-3}. The density at r = 7.5 cm was 2.3×10^9 cm^{-3}. If the density decay can be assumed to be exponential in the scrape-off layer, the density at the plasma edge is 1.4×10^{12} cm^{-3} and the e-folding length is 1.2 cm. During the ICRF heating, the gradient of electorn density in the scrape-off layer increases (see Table 2). As is mentioned in Section 3.3, the increase of the density is partly due to oxygen contamination. The relative increase in T_{es} with rf heating is of great importance because it is possibly one of the causes of the reduction of hydrogen recycling of the limiter and of the impurity increase during the rf heating.

4. CONCLUSIONS

1. Limiters are the major sources of metallic and carbon impurities both in Ohmic heating and rf heating. The radiation from impurity ions originated from the limiter surface increases strongly with injected rf power. The plasma behavior was affected by impurities released from stainless steel limiter.

2. Faraday shield of the ICRF antenna is less important as impurity source than the limiter.

3. Using graphite limiters, contamination of the plasma with metal impurities was significantly reduced, which resulted in an improvement of the parameters in Ohmically heated plasmas. However, the increase of oxygen impurity during rf heating was so large that it limited the maximum rf power which could be delivered without disruption. There is an indication that the graphite limiter is the source of oxygen impurities during the rf heating.

4. With the stainless steel limiter, increase of OII radiation by rf heating is large in the vicinity of the antenna. This may be due to a local increase of the flux of energetic charge-exchange neutrals.

5. It has been found that the H_α + D_α radiation at the main limiter decreases with rf heating. This is probably due to change in recycling at the limiter surface. The main reason of

the change in recycling may be the observed increase of electron temperature during the rf heating. This has probably a close relation to oxygen-impurity on the graphite limiters.

ACKNOWLEDGMENTS

The authors are indebted to Messrs. S. Ishiguro and M. Mugishima for their assistance on JIPP T-IIU operation. The authors are also grateful to Professor A. Miyahara and Dr. K. Akaishi for their stimulating discussions.

REFERENCES

1) T. Amano et al., in Plasma Physics and Controlled Nuclear Fusion Research (Proc. 9th Int. Conf. Baltimore, 1982) Vol.I, IAEA, Vienna (1983) 219.

2) D. Hwang et al., *ibid.*, 3.

3) H. Kimura et al., in Plasma Physics and Controlled Nuclear Fusion Research (Proc. 8th Int. Conf. Brussels, 1980) Vol.II, IAEA, Vienna (1981) 105.

4) Equipe TFR, *ibid.*, 75.

5) S. Suckewer, E. Hinnov et al., Nucl. Fusion 21 (1981) 981.

6) R. Behn, A. de Chambrier et al., Plasma Physics and Controlled Fusion 26 (1984) 173.

7) J. Hosea et al., Proc. 4th Internal Symposium on Heating in Toroidal Plasmas, Rome (1984), to be published.

FIGURE CAPTIONS

Fig.1 Plan view of the JIPP T-IIU.

Fig.2 Sectional view of the vacuum vessel.

Fig.3 Intensity of impurity radiations as a function of rf power. Open circle is the radiation intensity with the SUS limiters and closed circle is that with the graphite limiter.

Fig.4 Change in oxygen and titanium radiations before and after titanium gettering. The rf power is 350 kW with P14 antenna. The first gettering is between shot Nos.10726 and 10727. After shot No.10735 the gettering was applied in every interval of discharge.

a) OV: 1) #10726, 2) #10727, 3) #10763

b) TiVIII: 1) #10713, 2) #10730, 3) #10766.

Fig.5 Toroidal variation of OII with rf heating. P6-P16 indicate location of the detectors.

a) 150 kW with P4 antenna.

b) 350 kW with P14 antenna.

Fig.6 Behavior of $H_\alpha + D_\alpha$, OII radiations, horizontal displacement Δh and vertical displacement Δv. The rf power is 220 kW with P4. The detector at P16 looks directly at the inner limiter at P17. The detector at P6 looks at 14-15 cm distant from the limiter at P7.

Fig.7 Electron temperature T_{es} and density n_{es} in the scrape-off layer as a function of the rf power at a distance of 6.5 cm from the plasma edge.

Table 1. Parameters of Ohmic plasmas and temperatures with ICRF. The power of rf is 500 kW for the SUS-limiter case and 250 kW for the graphite-limiter case.

		SUS limiter	C limiter
Toroidal field	B_o	2.94 T	2.94 T
Plasma current	I_p	170 kA	240 kA
Loop voltage	V_l	4.0 V	2.5 V
Ohmic input		680 kW	600 kW
Line averaged electron density			
	(x 10^{13} cm^{-3})	2.5	3.5
Central electron Temperature $T_e(0)$			
	without ICRF	700 eV	1100 eV
	with ICRF	1100 eV	1800 eV
Central ion temperature $T_i(0)$			
	without ICRF	400 eV	400 eV
	with ICRF	1100 eV	800 eV

Table 2. Electron density n_{es} and T_{es} in the scrape-off layer with graphite limiters. Parameters of Ohmic plasma are shown in Table 1. The input power of ICRF is 220 kW.

	Ohmic heating		ICRF heating	
	6.5 cm	7.5 cm	6.5 cm	7.5 cm
n_{es} (x 10^{10} cm^{-3})	0.54	0.23	7.8	1.9
T_{es} (eV)	9.2	6.4	19.2	11.8

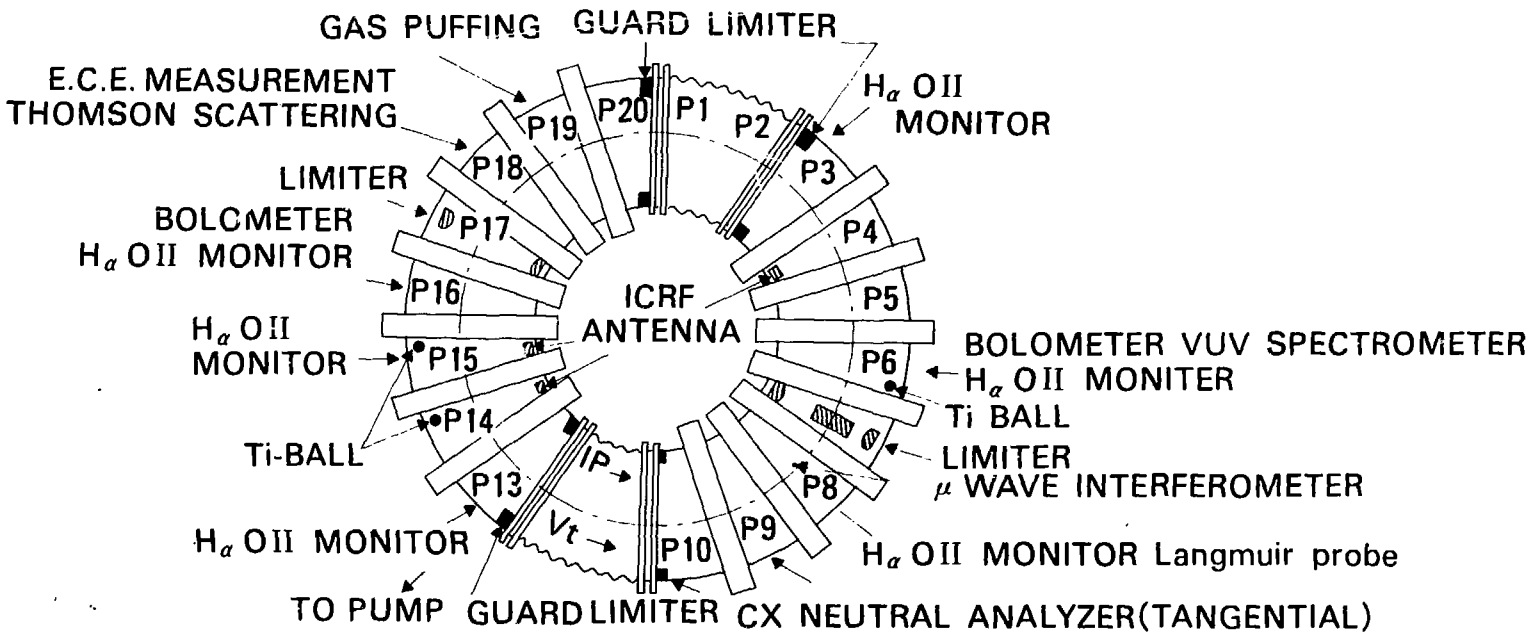
GAS PUFFING
GUARD LIMITER
E.C.E. MEASUREMENT
THOMSON SCATTERING
H_α OII
MONITOR
LIMITER
BOLOMETER
H_α OII MONITOR
ICRF
ANTENNA
H_α OII
MONITOR
BOLOMETER VUV SPECTROMETER
H_α OII MONITER
Ti BALL
LIMITER
μ WAVE INTERFEROMETER
Ti-BALL
IP
Vt
H_α OII MONITOR
H_α OII MONITOR Langmuir probe
TO PUMP
GUARD LIMITER
CX NEUTRAL ANALYZER(TANGENTIAL)
P1
P2
P3
P4
P5
P6
P8
P9
P10
P13
P14
P15
P16
P17
P18
P19
P20

FIG. 1

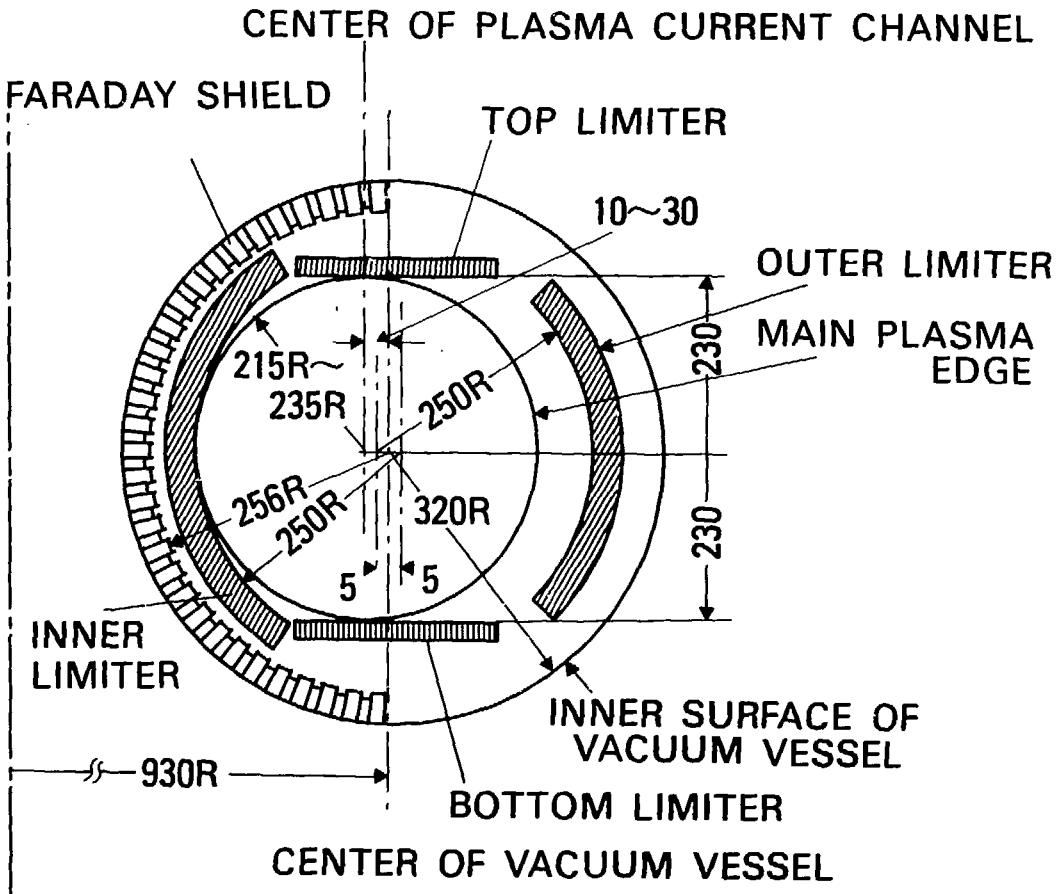
CENTER OF PLASMA CURRENT CHANNEL
FARADAY SHIELD
TOP LIMITER
10~30
OUTER LIMITER
MAIN PLASMA EDGE
215R~235R
250R
256R
250R
320R
5
5
230
230
INNER LIMITER
INNER SURFACE OF VACUUM VESSEL
930R
BOTTOM LIMITER
CENTER OF VACUUM VESSEL

FIG. 2

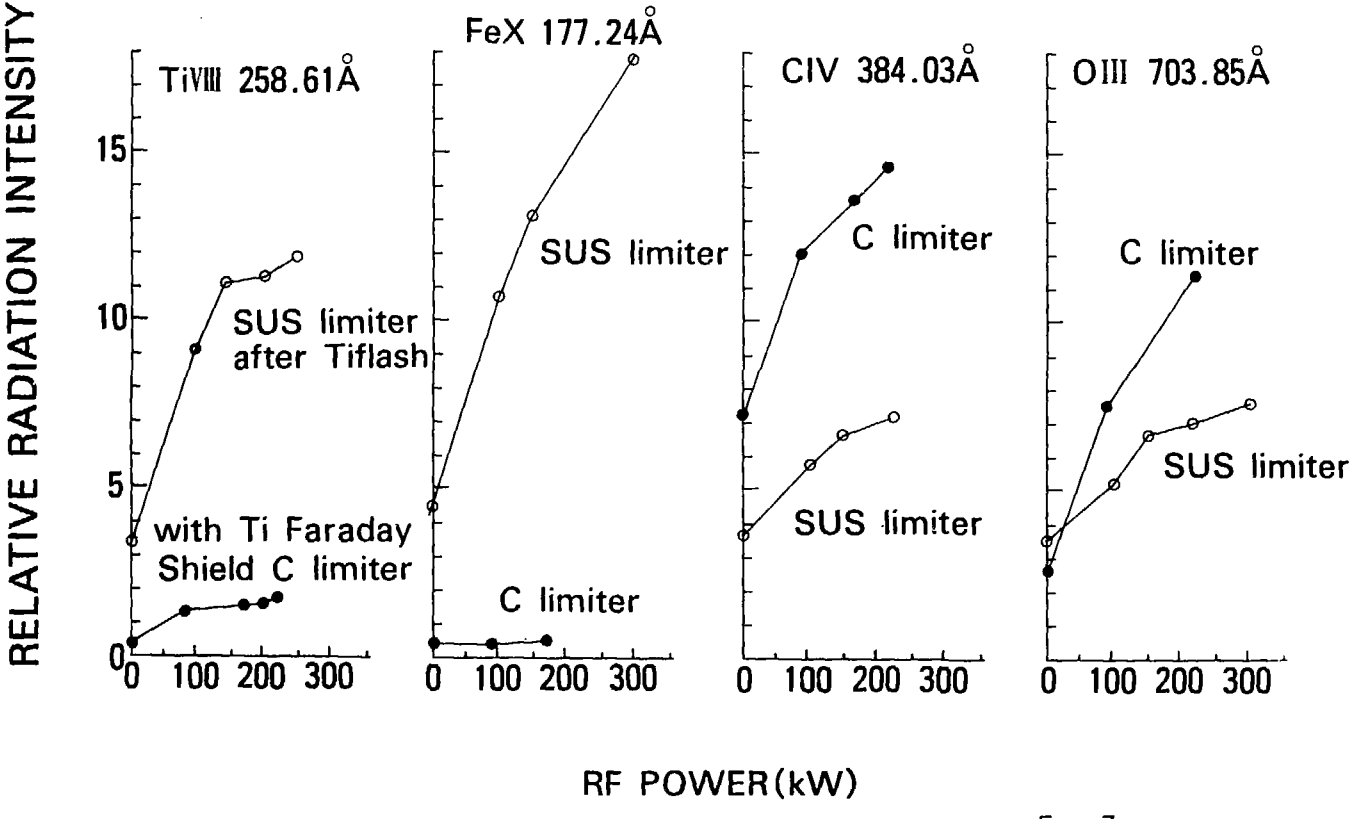
RELATIVE RADIATION INTENSITY
TiVIII 258.61Å
FeX 177.24Å
CIV 384.03Å
OIII 703.85Å
SUS limiter after Tiflash
with Ti Faraday Shield C limiter
SUS limiter
C limiter
C limiter
SUS limiter
C limiter
SUS limiter
0
5
10
15
0 100 200 300
RF POWER(kW)

FIG. 3

350kW with P14 antenna

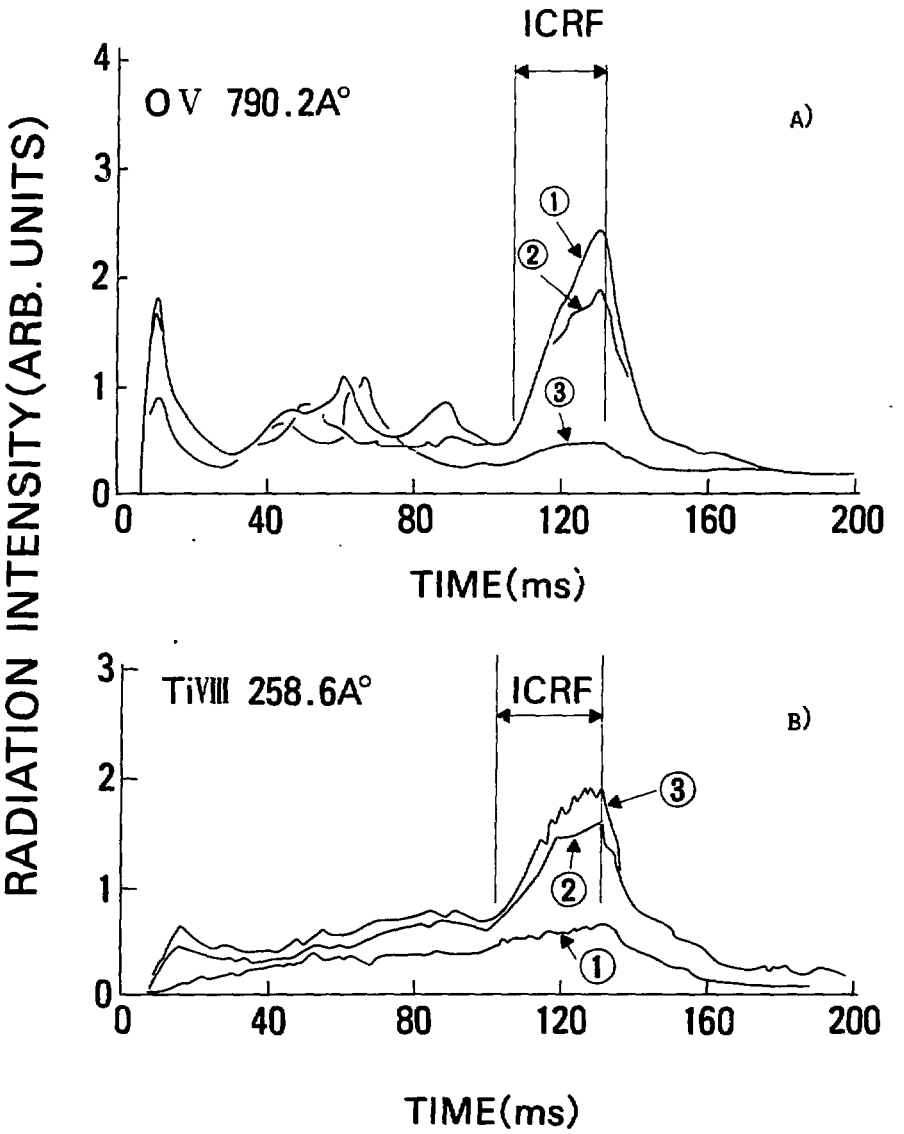

FIG. 4

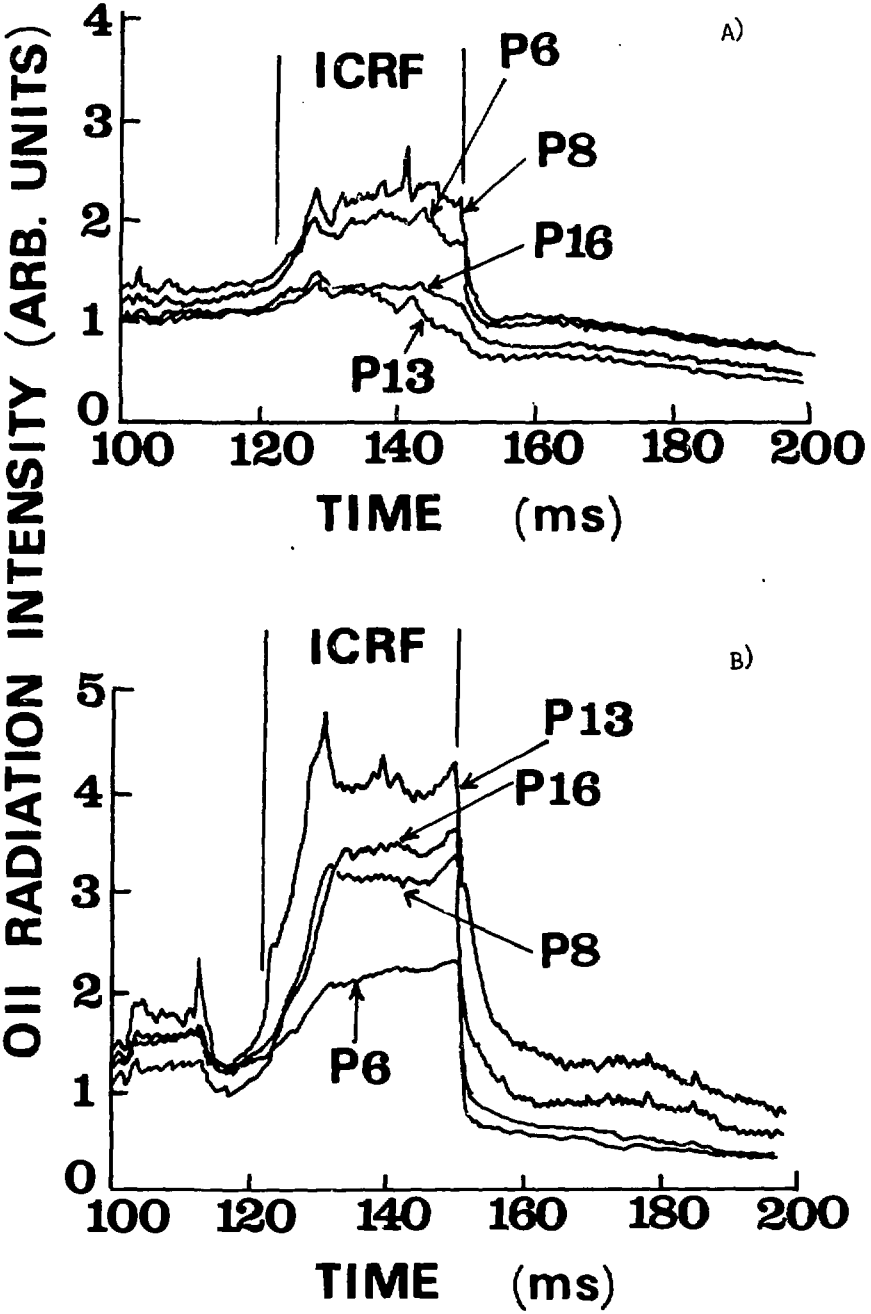
A)
ICRF
P6
P8
P16
P13
OII RADIATION INTENSITY (ARB. UNITS)
0
1
2
3
4
100
120
140
160
180
200
TIME (ms)
B)
ICRF
P13
P16
P8
P6
0
1
2
3
4
5
100
120
140
160
180
200
TIME (ms)

FIG. 5

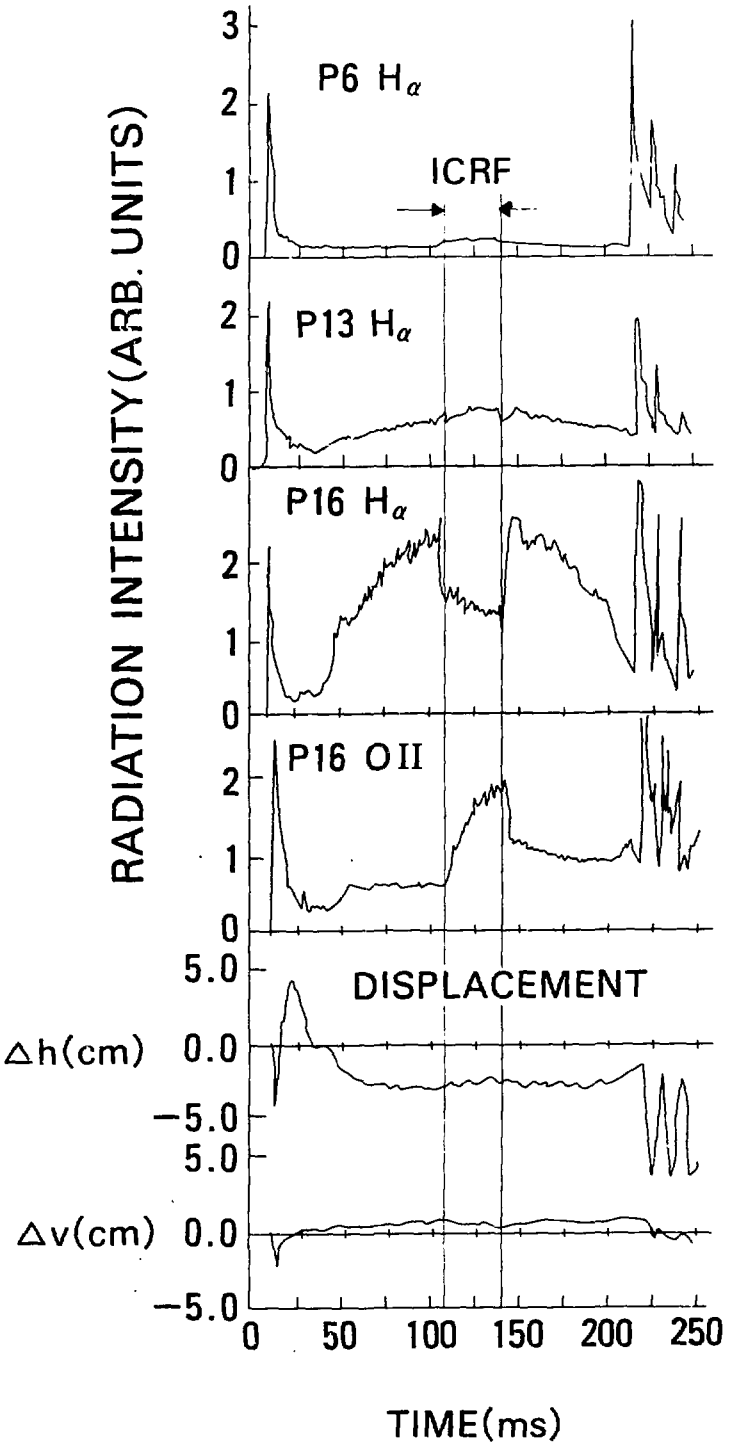
RADIATION INTENSITY(ARB. UNITS)
P6 Hα
ICRF
P13 Hα
P16 Hα
P16 OII
DISPLACEMENT
Δh(cm)
Δv(cm)
5.0
0.0
−5.0
5.0
0.0
−5.0
0
50
100
150
200
250
TIME(ms)

FIG. 6

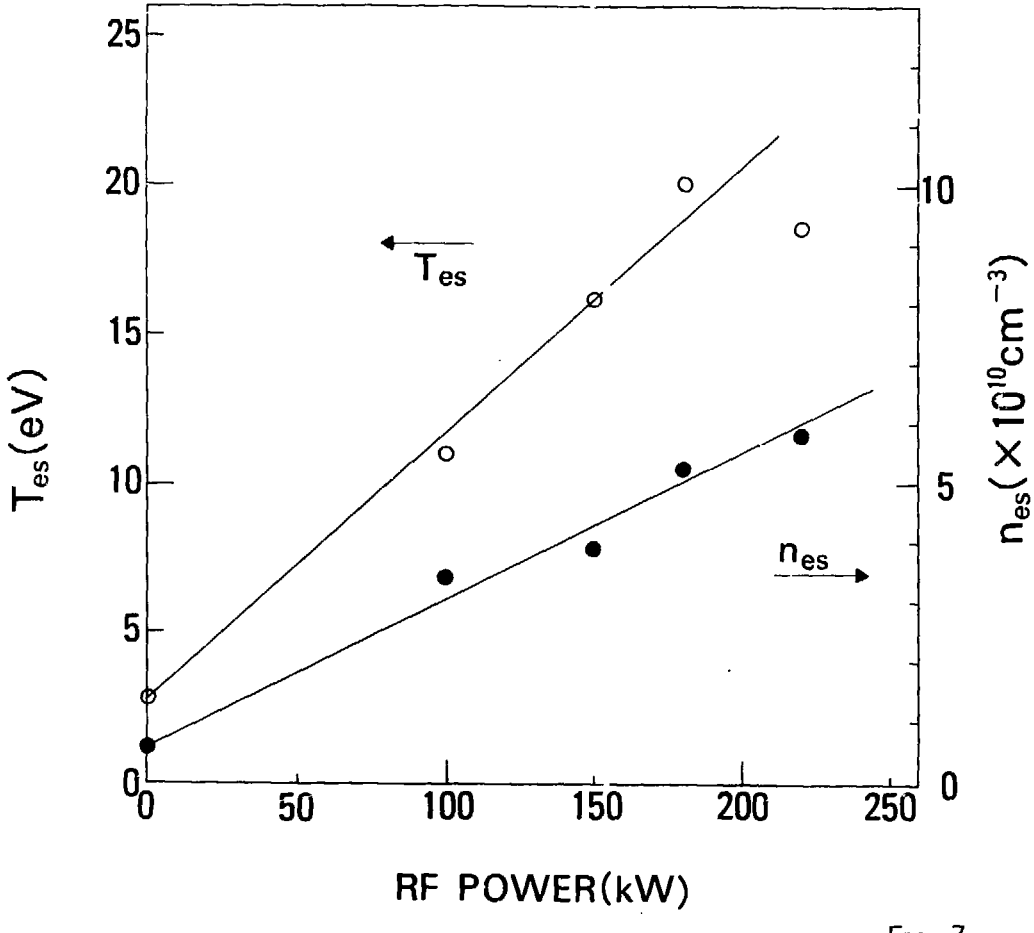
25
20
15
10
5
0
0
50
100
150
200
250
10
5
0
T_{es}
T_{es}(eV)
n_{es}
n_{es}($\times 10^{10}$cm^{-3})
RF POWER(kW)

FIG. 7